

1           **Association of Complement C3 Inhibitor Pegcetacoplan**  
2           **with Photoreceptor Degeneration Beyond Areas of**  
3           **Geographic Atrophy**

4   Maximilian Pfau, MD<sup>1,2,3</sup>; Steffen Schmitz-Valckenberg, MD<sup>1,2,4</sup>; Ramiro Ribeiro, MD, PhD<sup>5</sup>;  
5   Reza Safaei, MD<sup>5</sup>; Alex McKeown, PhD, MBA<sup>5</sup>; Monika Fleckenstein, MD<sup>2,4</sup>; Frank G. Holz,  
6   MD<sup>1,2</sup>

- 7           1. Department of Ophthalmology, University of Bonn, Bonn, Germany  
8           2. GRADE Reading Center, Bonn, Germany  
9           3. Institute of Molecular and Clinical Ophthalmology Basel, Basel, Switzerland  
10          4. John A. Moran Eye Center, University of Utah, Salt Lake City, USA  
11          5. Apellis Pharmaceuticals, Waltham, Massachusetts, USA

12 **Running Head:**           Association of pegcetacoplan therapy with photoreceptor degeneration

13 **Keywords:**               Age-related macular degeneration, junctional zone, outer retinal  
14                                degeneration, progression, optical coherence tomography

15 **Word count:**               3,132

16 **Figures:**                   3

17 **Tables:**                     2

18 **Supplementary Figures:**   7

19 **Supplementary Tables:**   5

20 **Corresponding author:**

21 Steffen Schmitz-Valckenberg, MD

22 Department of Ophthalmology & Visual Sciences

23 John A. Moran Eye Center

24 University of Utah

25 65 North Mario Capecchi Drive

26 Salt Lake City, UT 84312, USA

27 Phone:           +1 801 585 5586

28 Mail:            [steffen.valckenberg@utah.edu](mailto:steffen.valckenberg@utah.edu)

29 **ABSTRACT**

30 Preservation of photoreceptors beyond areas of retinal pigment epithelium atrophy is a  
31 critical treatment goal in eyes with geographic atrophy (GA) to prevent vision loss. Thus, we  
32 assessed the association of treatment with the complement C3 inhibitor pegcetacoplan with  
33 optical coherence tomography (OCT)-based photoreceptor laminae thicknesses in this post  
34 hoc analysis of the FILLY trial (NCT02503332).

35 Retinal layers in OCT were segmented using a deep-learning-based pipeline and extracted  
36 along evenly spaced contour-lines surrounding areas of GA. The primary outcome measure  
37 was change from baseline in (standardized) outer nuclear layer (ONL) thickness at the 5.16°-  
38 contour-line at month 12.

39 Participants treated with pegcetacoplan monthly had a thicker ONL along the 5.16° contour-  
40 line compared to the pooled sham arm (mean difference [95% CI] +0.29 z-score units [0.16,  
41 0.42],  $P < .001$ ). The same was evident for eyes treated with pegcetacoplan every other month  
42 (+0.26 z-score units [0.13, 0.4],  $P < .001$ ). Additionally, eyes treated with pegcetacoplan  
43 exhibited a thicker photoreceptor inner segment layer along the 5.16°-contour-line at  
44 month 12.

45 These findings suggest that pegcetacoplan could slow GA progression and lead to a lesser  
46 thinning of photoreceptor layers beyond the GA boundary. Future trials in earlier disease  
47 stages, i.e., intermediate AMD, aiming to slow photoreceptor degeneration warrant  
48 consideration.

## 49 INTRODUCTION

50 Geographic atrophy (GA), the atrophic late-stage manifestation of age-related macular  
51 degeneration, is a leading cause of legal blindness in industrialized countries.<sup>1–3</sup> To date, no  
52 treatment options – beyond low vision aids – are available. Multiple complement inhibitors  
53 are currently evaluated in clinical trials. These include pegcetacoplan (APL-2), which slowed  
54 GA progression in recent Phase 2 and 3 trials.<sup>4–6</sup>

55 The defining lesions of GA are foci of retinal pigment epithelium (RPE), photoreceptor, and  
56 choriocapillaris atrophy that progress and fuse over time.<sup>7</sup> The area of these lesions is  
57 associated with a corresponding visual function loss,<sup>8,9</sup> impairment of activities of daily  
58 living,<sup>10</sup> and reduced quality of life.<sup>11,12</sup> Thus, the total area of RPE-atrophy has served as the  
59 primary outcome measure in multiple trials.

60 However, eyes with GA are also affected by photoreceptor degeneration beyond areas of  
61 RPE-atrophy. This photoreceptor degeneration is observable as localized thinning of the  
62 outer nuclear layer (ONL) in the so-called junctional zone (500  $\mu\text{m}$  band surrounding GA).<sup>13,14</sup>  
63 In addition, photoreceptor degeneration may be more widespread, especially in association  
64 with subretinal drusenoid deposits (SDD, or reticular pseudodrusen).<sup>15–17</sup> This more diffuse  
65 form of outer retinal degeneration can be quantified as an outer nuclear layer (ONL),  
66 photoreceptor inner segment (IS), and outer segment (OS) thinning in eyes with intermediate  
67 AMD,<sup>17–19</sup> and GA.<sup>14,20–22</sup> Importantly, thinning at the level of the ONL is an established  
68 surrogate of impaired light sensitivity.<sup>17–19,23</sup> A recent analysis showed that treatment with  
69 pegcetacoplan is associated with less thinning between the inner boundary of the ellipsoid  
70 zone and the outer boundary of band three. However, data on the ONL and differential data  
71 for the IS and OS layers are lacking to date.<sup>24</sup>

72 Thus, we aimed to assess the association of pegcetacoplan treatment with the change  
73 individual photoreceptor laminae thicknesses in patients with GA secondary to AMD. The  
74 presented analysis using data from the FILLY phase 2 trial (ClinicalTrials.gov identifier  
75 NCT02503332) fully accounts for the normal spatial variation in photoreceptor laminae

- 76 thicknesses aiming to evaluate photoreceptor degeneration independent of the changes  
77 related to mere differences in RPE-atrophy progression rates.

## 78 **RESULTS**

### 79 *Cohort*

80 Forty-nine of the 246 clinical trial participants were excluded since they underwent spectral-  
81 domain optical coherence tomography (SD-OCT) imaging using a Cirrus device  
82 (Supplementary Figure S1).

83 A total of 197 participants were imaged with a Heidelberg Spectralis OCT device, of whom  
84 192 had follow-up imaging data available and met the prespecified modified intention-to-treat  
85 (mITT) criteria for analysis (i.e., 97.5 % of the participants imaged with a Heidelberg  
86 Spectralis OCT device, and 78 % of all randomized participants). The participants  
87 (female: 122 [63.5%]; male: 70 [36.5%]) had a mean age of 79.4 years (SD: 7.53; range:  
88 60.0 to 97.0) at baseline with a mean (autofluorescence based) sqrt-transformed area of  
89 fundus autofluorescence (FAF)-based RPE-atrophy of 2.80 mm (SD: 0.718; range: 1.59,  
90 4.16). The three study arms had no distinct differences (Table 1).

91 Participants enrolled at clinical sites using the Cirrus device, which could not be included in  
92 this analysis, were well-aligned with the included participants from sites using the Spectralis  
93 device (Supplementary Table S1)

### 94 *Segmentation Accuracy*

95 To assess the accuracy of the segmentation pipeline, we compared our SD-OCT-derived  
96 measurement of the area of RPE-atrophy (cf., Figure 1) with the previously reported FAF-  
97 based measurement of RPE-atrophy. For the subset of study eyes with measurable RPE-  
98 atrophy (i.e., RPE-atrophy within the SD-OCT image frame), there was no relevant difference  
99 (systematic bias) between the original FAF-based measurements and the SD-OCT derived  
100 data (bias estimate [95% CI] of 0.02 mm [0.00; 0.05]. P=0.020, Supplementary Figure S2).

101 *SD-OCT-based Trial Outcome*

102 The primary outcome measure for the SD-OCT-based assessment mirrored the previous  
103 FAF-based report. Specifically, for the subset of study eyes with GA within the image frame  
104 ( $n = 135$ ), the square-root transformed atrophy progression was slower by 25% in eyes  
105 treated with pegcetacoplan monthly (sham - pegcetacoplan monthly estimate:  $+0.076$  mm/y,  
106 SE: 0.038,  $P=0.0473$ ), and in eyes treated with pegcetacoplan every other month (EOM)  
107 22.2% (sham pooled - pegcetacoplan EOM estimate:  $+0.068$  mm/y, SE: 0.04,  $P=.09$ ).

108 *Photoreceptor Layer Thickness Outside of GA*

109 At baseline, all three arms (sham pooled, pegcetacoplan monthly, and pegcetacoplan EOM)  
110 exhibited similar degrees of photoreceptor thinning. Specifically, the ONL was thinned in the  
111 immediate junctional zone, with a steep gradient between  $0^\circ$  to  $2^\circ$  [approx. 0 to 582  $\mu\text{m}$ ] from  
112 the boundary of RPE-atrophy and a less steep gradient at more eccentric locations (Figure  
113 2). Similarly, marked IS and OS thinning was evident outside of RPE-atrophy across all  
114 groups at baseline (Supplementary Figure S3).

115 *Change in Photoreceptor Layer Thickness Over Time*

116 At month 12, eyes treated with pegcetacoplan exhibited a lesser degree of progressive  
117 thinning at the level of the ONL along their new junctional zone compared to eyes in the  
118 sham arm. Specifically, the ONL along the  $5.16^\circ$  contour-line was markedly thicker compared  
119 to sham in the pegcetacoplan monthly group (contrast estimate [95% CI] for pegcetacoplan  
120 monthly - sham:  $+0.29$  z-score units [0.16, 0.42],  $P<.001$ ) and in the pegcetacoplan EOM  
121 group (pegcetacoplan EOM - sham:  $+0.26$  z-score units [0.13, 0.4],  $P<.001$ ).

122 Likewise, the retina at the level of the IS layer was also thicker in both treatment arms  
123 compared to sham at month 12 along the  $5.16^\circ$  contour-line (pegcetacoplan monthly - sham:  
124  $+0.42$  z-score units [0.21, 0.62],  $P<.001$ ; pegcetacoplan EOM sham:  $+0.34$  z-score units  
125 [0.12, 0.55],  $P<.001$ ). The same was observed for the  $2.58^\circ$  contour-line (Table 2,  
126 Supplementary Figure S4).

127 At the level of the OS layer, the results were overall indistinct (Table 2). The OS layer  
128 differed at month 12 only along the 2.58° contour-line markedly in thickness in the  
129 pegcetacoplan EOM group compared to sham (pegcetacoplan EOM - sham: +0.52 z-score  
130 units [0.21, 0.83],  $P < .001$ ).

131 Analysis of the change over time (Figure 3), revealed for the ONL and IS less thinning at the  
132 level of the photoreceptors with increasing duration of treatment (i.e., estimate at month 12  
133 and 6 > month 2) and with more frequent dosing (estimates for pegcetacoplan monthly >  
134 pegcetacoplan EOM). Notably, these differences were evident through month 18. The PP  
135 analysis (Supplementary Table S2, Supplementary Figure S5) and the PP analysis excluding  
136 all visits from eyes with exudation at any time point (Supplementary Table S3,  
137 Supplementary Figure S6) confirmed these results with even larger coefficients.

#### 138 *Association of Pegcetacoplan with Fellow Eye Photoreceptor Thickness*

139 Fellow eye data (eyes without macular neovascularization and a baseline RPE-atrophy area  
140  $\geq 2.5 \text{ mm}^2$ ) were available for 112 participants (eligible fellow eyes per arm: sham N=41,  
141 pegcetacoplan monthly N=33, pegcetacoplan EOM N=38). Applying the same contour-line-  
142 based analysis in these eyes yielded similar results concerning baseline thinning of the ONL,  
143 IS, and OS in the junctional zone. However, there were no longitudinal changes in the fellow  
144 eyes of all three arms (Supplementary Table S4, Supplementary Figure S7).

## 145 **DISCUSSION**

146 This study analyzed the impact of the C3 inhibitor pegcetacoplan on photoreceptor  
147 degeneration outside of RPE-atrophy using data from the randomized FILLY phase-2 trial.  
148 Specifically, we demonstrated that eyes treated with pegcetacoplan exhibit a lesser degree  
149 of thinning at the level of photoreceptors outside of RPE-atrophy at the end of the study  
150 compared to eyes in the sham arm.

151 The area of RPE-atrophy has been established as the primary structural endpoint to quantify  
152 disease progression in eyes with GA.<sup>2</sup> For this purpose, RPE-atrophy is well suited since it  
153 represents the boundary of deep scotomata in eyes with GA as shown by fundus-controlled  
154 perimetry studies,<sup>8,26</sup> is prognostic for reading ability,<sup>27–29</sup> as for quality of life.<sup>11,27</sup> While early  
155 studies typically used fundus photography for the quantification of the area of RPE-atrophy,<sup>30</sup>  
156 FAF-based quantification using semiautomated software such as the RegionFinder software  
157 (Heidelberg Engineering, Germany) is currently the gold standard used in large-scale clinical  
158 trials<sup>31–33</sup> More recently, GA quantification with other semi and fully automated approaches  
159 for FAF or OCT data has been proposed.<sup>34–37</sup> However, the area of RPE-atrophy depicts only  
160 partially the severity of AMD in a patient with GA.

161 In the setting of intermediate AMD and GA, it is now established that photoreceptors –  
162 especially in association with SDD – show degenerative changes over time in a macula-wide  
163 manner.<sup>15,17,20,21,38</sup> Importantly, histopathologic data are congruent with photoreceptor  
164 degeneration distant to the boundary of RPE-atrophy,<sup>14</sup> and suggest that rod photoreceptor  
165 degeneration precedes cone degeneration in AMD.<sup>39,40</sup> Therefore, treatment of the non-  
166 exudative component of AMD should ideally address not only RPE-atrophy but also  
167 photoreceptor degeneration in the broader sense. Thus, we have analyzed the association of  
168 pegcetacoplan with photoreceptor degeneration outside of RPE-atrophy.

169 Interestingly, the analyses for all three photoreceptor laminae demonstrated that  
170 pegcetacoplan was associated with less thinning at the level of photoreceptors outside areas



171 of RPE-atrophy. Considering Bradford Hill's criteria for causation,<sup>41</sup> the here observed  
172 associations may be causal. First and foremost, the association strength is substantial,  
173 follows a plausible temporal sequence (estimate increases over time), and shows a biological  
174 gradient (dose-response relationship with a more substantial impact for eyes treated monthly  
175 instead of EOM). Moreover, the association is specific, as evidenced by the absence of an  
176 association in the fellow eyes. Since photoreceptor thinning correlates closely to impaired  
177 light sensitivity,<sup>17,19,42-44</sup> it is possible that the observed changes are functionally beneficial.

178 Overall, the results shown here align with the previous analysis by Sophie Riedl and  
179 coworkers.<sup>24</sup> Through differential analysis of all three photoreceptor laminae, our data  
180 suggests that their observed effect (based on a combined IS+OS layer definition) is  
181 predominantly attributable to changes at the IS level. Importantly, our analysis fully  
182 accounted for the spatial variation in photoreceptor laminae thickness through  
183 standardization. Thus, our results attest that the preservation of photoreceptor laminae  
184 thickness in the junctional zone can not be attributed to an overall less eccentric junctional  
185 zone in treated eyes at month 12 due to the slower RPE-atrophy progression. Instead, the  
186 observation presents a genuine lesser degree of photoreceptor thinning independent of the  
187 underlying RPE-atrophy progression.

188 As a related concept, Wu and coworkers have proposed 'nascent GA', a combination of OCT  
189 imaging signs preceding RPE-atrophy, as an endpoint applicable to evaluate retinal  
190 degeneration in eyes with intermediate AMD,<sup>45</sup> and demonstrated its prognostic value.<sup>46</sup> This  
191 concept was more recently incorporated by the Classification of Atrophy Meeting (CAM)  
192 consortium as a part of incomplete RPE and outer retinal atrophy (iRORA).<sup>47,48</sup> Besides  
193 incident iRORA (or nGA) as an endpoint, the rate of iRORA to RPE-atrophy transition distant  
194 to the junctional zone has been proposed as an endpoint.<sup>49</sup> In another post-hoc study of the  
195 FILLY trial, a reduced iRORA to RPE-atrophy transition rate in eyes treated with  
196 pegcetacoplan was reported.<sup>50</sup> Further studies are warranted to examine whether the

197 observed lesser thinning at the level of the ONL along contour-lines reflects the sum of  
198 decreased focal thinning primarily,<sup>50</sup> or reduced thinning in a ‘macula-wide’ manner.

### 199 *Limitations*

200 This analysis was a post-hoc study. Accordingly, the results must be considered hypothesis-  
201 generating rather than confirming.

202 The approach of using ‘traveling’ contour-lines (after standardization of the thickness data)  
203 entails assumptions. This includes the absence of spatial patterns of (marked) photoreceptor  
204 degeneration unrelated to the junctional zone. The relative stability (or trend toward slight  
205 thinning) of the junctional zone photoreceptor thicknesses over time in the here presented  
206 fellow eye data and previous natural-history data implies that these assumptions are met.<sup>20</sup>

207 Notably, functional evidence will be needed to demonstrate genuine photoreceptor protection  
208 with absolute certainty (instead of the unlikely case of subtle thickening due to other  
209 causes).<sup>51</sup> There is no evidence that the here observed findings are a result of ‘pre- or  
210 subclinical exudation’, given that the analysis excluding all visits from eyes that developed  
211 exudation at any time point showed consistent results (Supplementary Table S3,  
212 Supplementary Figure S6).

213 It is unclear why IS thickness showed the most distinct change in treated eyes.

214 Histopathologic data would suggest that both IS and OS thickness are suitable biomarkers  
215 for photoreceptor integrity. In contrast, ONL thickness is partially confounded by HFL.<sup>14</sup>

216 Ultrahigh-resolution OCT technology would most likely provide more precise estimates of  
217 change-over-time in IS and OS thickness given the greater axial resolution.<sup>52</sup> Last, analysis  
218 of photoreceptor degeneration outside of RPE-atrophy in the larger phase 3 trials  
219 investigating the same drug is warranted (i.e., DERBY, OAKS) and across investigational  
220 drugs (including among other avacincaptad pegol,<sup>53</sup> IONIS-FB-LRx,<sup>54</sup> FHTR2163<sup>55</sup>).

221 **CONCLUSION**

222 In summary, this post-hoc analysis of the FILLY trial showed that treatment with  
223 pegcetacoplan was associated with less outer retinal thinning over time in a dose-dependent  
224 manner. Specifically, eyes treated with monthly pegcetacoplan (compared to controls)  
225 exhibited at month 12 relatively more intact tissue at the level of the ONL, IS, and OS  
226 laminae outside of the RPE-atrophy junctional zone. These results may support a therapeutic  
227 effect of pegcetacoplan on photoreceptors in eyes with GA.

## 228 **METHODS**

### 229 *Clinical Trial Data*

230 This post-hoc analysis was conducted between August 2021 and February 2022 and based  
231 on data acquired previously in the FILLY trial and is reported with adherence to the  
232 CONSORT standard. The protocol has been described previously (study start date:  
233 September 24, 2015, primary completion date: July 14, 2017).<sup>5</sup> Ethics approval was obtained  
234 from all necessary boards, written informed consent was obtained from all participants, and  
235 participants did not receive a stipend.<sup>5</sup> Sex was self-reported.

236 FILLY was a multicenter, randomized, single-masked, sham-controlled study to assess the  
237 safety of pegcetacoplan in patients with GA secondary to AMD. Study participants had to  
238 have a total GA area  $\geq 2.5$  mm<sup>2</sup> (with one focus of GA  $\geq 1.25$  mm<sup>2</sup> in eyes with multifocal GA)  
239 and  $\leq 17.5$  mm<sup>2</sup> as assessed by fundus autofluorescence imaging. A total of 246 participants  
240 were included and randomized in a 2:2:1:1 manner to pegcetacoplan monthly,  
241 pegcetacoplan every other month (EOM), sham monthly, or sham EOM.<sup>5</sup>

242 Study participants in the monthly group received pegcetacoplan (or sham) injections and  
243 study procedures monthly until month 12. Participants in the EOM groups received  
244 pegcetacoplan (or sham) injections every two months until month 12. In addition, all  
245 participants were imaged at a month 15 and month 18 follow-up visit (3 and 6 months after  
246 the last injection, respectively).<sup>5</sup>

### 247 *Imaging Data*

248 Besides fundus autofluorescence (FAF) imaging, participants underwent (among other  
249 imaging modalities) SD-OCT imaging, either with a Spectralis device (20°x20°, 49 B-scans,  
250 N=197 participants, Heidelberg Engineering, Heidelberg, Germany) or with a Cirrus device  
251 (N=49 participants, Carl Zeiss Meditec, Jena, Germany). The first group (i.e., participants  
252 imaged with a Spectralis device) was included in this analysis (Supplementary Figure S1).  
253 Data from five participants were excluded due to lack of follow-up or deviation from the SD-

254 OCT protocol. Data acquired with the Cirrus device were excluded due to the lower axial  
255 resolution.

#### 256 *Prespecified Study Population and Pooling of the Sham Arms*

257 In analogy to the prespecified analysis of the primary endpoint,<sup>5</sup> the modified intention-to-  
258 treat (mITT) population included all participants with at least one injection and at least one  
259 follow-up examination at month 2 (or later) at which efficacy data were collected. The per-  
260 protocol (PP) population included all participants from the mITT population that did receive  
261 no less than 75% of their expected injections before month 12 (i.e., no less than nine  
262 [monthly group] or four injections [EOM group]) and the participants that did not receive the  
263 incorrect medication throughout the study. We also report the results for the PP population,  
264 excluding all visits from eyes that developed exudation at any time point. Both sham arms  
265 were pooled for the analyses.<sup>5</sup>

#### 266 *Image Data Segmentation and Standardization*

267 A previously validated convolutional neural network (CNN)<sup>20</sup> was applied to segment the  
268 retinal layers (cf., eMethods for layer definitions and segmentation methods). For the primary  
269 analyses, we compared photoreceptor laminae distances at fixed distances to the boundary  
270 of GA across time. Since these contour-lines ‘traveled’ with GA progression, all OCT  
271 thickness data were standardized to account for the normal topographic difference in  
272 photoreceptor laminae thickness and the effect of age. Specifically, we subtracted for each  
273 A-scan in the en-face maps the age-adjusted normal value of a given layer thickness and  
274 divided that value by the normal location-specific standard deviation (i.e., transformation to z-  
275 score units). This process has been described previously in detail.<sup>20</sup>

#### 276 *Feature Extraction*

277 The mean thickness values for the three photoreceptor laminae (ONL, IS, OS) were  
278 extracted along evenly spaced contour-lines around the lesions of GA (width: 0.43° [126 µm

279 in an emmetropic eye]).<sup>20</sup> The statistical analyses were performed for three representative  
280 contour-lines (distances to the GA boundary: 0.43°, 2.58°, and 5.16° [126 µm, 751 µm, and  
281 1502 µm in an emmetropic eye]). These evenly spaced contour-lines were derived through  
282 dilation of the initial segmentation of GA. Outer contour-lines could be discontinuous due to  
283 the image-frame. Notably, the contour-lines were defined on the current (i.e., same visit date)  
284 position of the GA boundary for all visits. This means that the counter-lines ‘traveled’ as the  
285 lesions expanded. The generated data are thus independent of the underlying rate of RPE-  
286 atrophy progression (i.e., not a mere representation of the slowed rate of GA progression  
287 with treatment). In the absence of treatment effects, there should be a slight thinning of  
288 photoreceptor laminae over time due to a subtle, ‘macula-wide’ component of photoreceptor  
289 degeneration.<sup>20</sup>

#### 290 *Statistical analyses*

291 The analyses were performed in the software environment R (version 4.1.0),<sup>56</sup> using the add  
292 on libraries dplyr (version 1.0.7),<sup>57</sup> ggplot2 (version 3.3.5),<sup>58</sup> lme4 (1.1-27.1),<sup>59</sup> and emmeans  
293 (version 1.6.2-1).<sup>60</sup>

294 The primary outcome measure was the between-group difference in change from baseline of  
295 the ONL thickness along the 5.16° contour-line at month 12. This distance was elected as  
296 the primary outcome measure to be genuinely independent of the junctional-zone component  
297 of GA. We also examined two additional contour-lines (0.43°, 2.58°, besides 5.16°), and fitted  
298 for each photoreceptor layer (ONL, IS, OS), a linear mixed model (LMM) based on the  
299 observed data (i.e., no imputation). The dependent variable was the change in layer  
300 thickness (z-score) from baseline, and the independent variables (fixed effects) were the  
301 treatment arm (pegcetacoplan monthly, pegcetacoplan EOM, and pooled sham), baseline  
302 layer thickness, visit (month 2, 6, 12, 18), and the treatment arms by visit interaction. The  
303 model included the patient ID as a random effect. The Kenward-Roger approximation was  
304 used to estimate the denominator degrees of freedom. P-values were adjusted for the three  
305 pairwise contrasts between the three groups (Tukey’s single-step multiple comparison

306 procedure). In this post-hoc analysis, estimates from a total of 27 LMMs are presented (3  
307 [contour-lines] x 3 [layers: ONL, IS, OS] x 3 [analyses: mITT, PP, fellow eyes]).

308 As an additional quality-control of the OCT segmentation, we performed an OCT-based  
309 analysis of the effect of pegcetacoplan on RPE-atrophy progression rates in analogy to the  
310 autofluorescence-based analysis in the original publication.<sup>5</sup> The change in square-root-  
311 transformed RPE-atrophy area from baseline was the dependent variable. The treatment arm  
312 (pegcetacoplan monthly, pegcetacoplan EOM, and pooled sham), baseline square-root-  
313 transformed RPE-atrophy area, visit (month 2, 6, 12, 18), and the treatment arms by visit  
314 interaction and the sqrt-baseline-area by visit interaction were included as the fixed effects.  
315 The model included the patient ID as a random effect. In addition, a Bland-Altman analysis  
316 was performed to compare the OCT and FAF data.<sup>61</sup>

317 **ADDITIONAL INFORMATION**

318 **Author Contributions**

319 All authors are responsible for conception and design of the study. MP, and SSV are  
320 responsible for the analysis of the data. All authors contributed to interpretation of data,  
321 drafting of the manuscript, critical revision of the manuscript, final approval of the manuscript.

322 **Competing interests**

323 **Funding:** This study was funded by Apellis Pharmaceuticals, Waltham, Massachusetts,  
324 USA.

325 Methods development relevant to this work was supported by a National Institutes of Health  
326 Core Grant (EY014800), and an Unrestricted Grant from Research to Prevent Blindness,  
327 New York, NY, to the Department of Ophthalmology & Visual Sciences, University of Utah,  
328 and the German Research Foundation (DFG) grant no.: PF950/1-1 (to MP), and FL658/4-1  
329 and FL658/4-2 (to MF).

330 **Financial Disclosures:**

331 **M. Pfau** reports personal fees from Apellis and Novartis outside the submitted work.

332 **S. Schmitz-Valckenberg** reports grants from Acucela/Kubota Vision, personal fees from  
333 Apellis, grants and personal fees from Novartis, grants and personal fees from Allergan,  
334 grants and personal fees from Bayer, grants and personal fees from Bioeq/Formycon, grants,  
335 personal fees and non-financial support from Carl Zeiss MediTec AG, grants and non-  
336 financial support from Centervue, personal fees from Galimedix, grants, personal fees and  
337 non-financial support from Heidelberg Engineering, grants from Katairo, non-financial support  
338 from Optos, personal fees from Oxurion, outside the submitted work.

339 **Ramiro Ribeiro** is employed by Apellis Pharmaceuticals, Waltham, Massachusetts, USA.

340 **Reza Safaei** is employed by Apellis Pharmaceuticals, Waltham, Massachusetts, USA.

341 **Alex McKeown** is employed by Apellis Pharmaceuticals, Waltham, Massachusetts, USA.



342 **M. Fleckenstein** reports grants, personal fees and non-financial support from Heidelberg  
343 Engineering, non-financial support from Zeiss Meditec, grants and non-financial support  
344 from Optos, personal fees and grant from Novartis, personal fees from Bayer, grants and  
345 personal fees from Genentech, from Roche, outside the submitted work; In addition, Dr.  
346 Fleckenstein is an inventor on a patent US20140303013 A1 pending.

347 **F.G. Holz** reports personal fees from Acucela, Apellis, Bayer, Boehringer-Ingelheim,  
348 Bioeq/Formycon, Roche/Genentech, Geuder, Graybug, Gyroscope, Heidelberg Engineering,  
349 IvericBio, Kanghong, LinBioscience, Novartis, Oxurion, Pixium Vision, Oxurion, Stealth  
350 BioTherapeutics, and Zeiss. Prof. Holz reports grants from Allergan, Apellis, Bayer,  
351 Bioeq/Formycon, CenterVue, Ellex, Roche/Genentech, Geuder, Heidelberg Engineering,  
352 IvericBio, Kanghong, NightStarX, Novartis, Optos, Pixium Vision, and Zeiss.

353 **Role of Sponsor:** The sponsor or funding organizations had no role in the conduct of the  
354 analysis but were involved in the interpretation of the data, preparation, review, and approval  
355 of the manuscript. The authors alone are responsible for the content and writing of the paper.  
356 The views expressed are those of the authors.

357 **Data Sharing:**

358 Original data will be shared from the corresponding authors upon reasonable request.

359

## 360 REFERENCES

- 361 1. Fleckenstein, M. et al. Age-related macular degeneration. *Nat. Rev. Dis. Prim.* **7**, 31  
362 (2021).
- 363 2. Schmitz-Valckenberg, S. et al. Geographic atrophy: Semantic considerations and  
364 literature review. *Retina* **36**, 2250–2264 (2016).
- 365 3. Holz, F. G., Strauss, E. C., Schmitz-Valckenberg, S. & Van Lookeren Campagne, M.  
366 Geographic atrophy: Clinical features and potential therapeutic approaches.  
367 *Ophthalmology* **121**, 1079–1091 (2014).
- 368 4. Hughes, S. et al. Prolonged intraocular residence and retinal tissue distribution of a  
369 fourth-generation compstatin-based C3 inhibitor in non-human primates. *Clin.*  
370 *Immunol.* **214**, 108391 (2020).
- 371 5. Liao, D. S. et al. Complement C3 Inhibitor Pegcetacoplan for Geographic Atrophy  
372 Secondary to Age-Related Macular Degeneration: A Randomized Phase 2 Trial.  
373 *Ophthalmology* **127**, 186–195 (2020).
- 374 6. Apellis Pharmaceuticals. *Apellis Announces Top-Line Results from Phase 3 DERBY*  
375 *and OAKS Studies in Geographic Atrophy (GA) and Plans to Submit NDA to FDA in*  
376 *the First Half of 2022.*
- 377 7. Fleckenstein, M. et al. The Progression of Geographic Atrophy Secondary to Age-  
378 Related Macular Degeneration. *Ophthalmology* **125**, 369–390 (2018).
- 379 8. Pfau, M. et al. Mesopic and Dark-Adapted Two-Color Fundus-Controlled Perimetry in  
380 Geographic Atrophy Secondary to Age-Related Macular Degeneration. *Retina* (2018).  
381 doi:10.1097/IAE.0000000000002337
- 382 9. Lindner, M. et al. Combined fundus autofluorescence and near infrared reflectance as  
383 prognostic biomarkers for visual acuity in foveal-sparing geographic atrophy. *Investig.*  
384 *Ophthalmol. Vis. Sci.* **58**, BIO61–BIO67 (2017).
- 385 10. Chakravarthy, U. et al. Characterizing Disease Burden and Progression of Geographic  
386 Atrophy Secondary to Age-Related Macular Degeneration. *Ophthalmology* **125**, 842–  
387 849 (2018).
- 388 11. Sivaprasad, S. et al. Reliability and Construct Validity of the NEI VFQ-25 in a Subset  
389 of Patients With Geographic Atrophy From the Phase 2 Mahalo Study. *Am. J.*  
390 *Ophthalmol.* **190**, 1–8 (2018).
- 391 12. Künzel, S. H. et al. Determinants of Quality of Life in Geographic Atrophy Secondary  
392 to Age-Related Macular Degeneration. *Invest. Ophthalmol. Vis. Sci.* **61**, 63 (2020).
- 393 13. Fleckenstein, M. et al. High-resolution spectral domain-OCT imaging in geographic  
394 atrophy associated with age-related macular degeneration. *Investig. Ophthalmol. Vis.*  
395 *Sci.* **49**, 4137–4144 (2008).
- 396 14. Li, M. et al. HISTOLOGY OF GEOGRAPHIC ATROPHY SECONDARY TO AGE-  
397 RELATED MACULAR DEGENERATION: A Multilayer Approach. *Retina* **38**, 1937–  
398 1953 (2018).
- 399 15. Spaide, R. F. Outer retinal atrophy after regression of subretinal drusenoid deposits as  
400 a newly recognized form of late age-related macular degeneration. *Retina* **33**, 1800–  
401 1808 (2013).
- 402 16. Chen, L. et al. SUBRETINAL DRUSENOID DEPOSIT IN AGE-RELATED MACULAR  
403 DEGENERATION: Histologic Insights Into Initiation, Progression to Atrophy, and  
404 Imaging. *Retina* **40**, 618–631 (2020).

- 405 17. Steinberg, J. S. *et al.* Correlation of Partial Outer Retinal Thickness with Scotopic and  
406 Mesopic Fundus-Controlled Perimetry in Patients with Reticular Drusen. *Am. J.*  
407 *Ophthalmol.* **168**, 52–61 (2016).
- 408 18. Gin, T. J., Wu, Z., Chew, S. K. H., Guymer, R. H. & Luu, C. D. Quantitative analysis of  
409 the ellipsoid zone intensity in phenotypic variations of intermediate age-related  
410 macular degeneration. *Investig. Ophthalmol. Vis. Sci.* **58**, 2079–2086 (2017).
- 411 19. Pfau, M. *et al.* Mesopic and dark-adapted two-color fundus-controlled perimetry in  
412 patients with cuticular, reticular, and soft drusen. *Eye* **32**, 1819–1830 (2018).
- 413 20. Pfau, M. *et al.* Progression of Photoreceptor Degeneration in Geographic Atrophy  
414 Secondary to Age-related Macular Degeneration. *JAMA Ophthalmol.* (2020).  
415 doi:10.1001/jamaophthalmol.2020.2914
- 416 21. Reiter, G. S. *et al.* Subretinal Drusenoid Deposits and Photoreceptor Loss Detecting  
417 Global and Local Progression of Geographic Atrophy by SD-OCT Imaging. *Invest.*  
418 *Ophthalmol. Vis. Sci.* **61**, 11 (2020).
- 419 22. Bird, A. C., Phillips, R. L. & Hageman, G. S. Geographic atrophy: A histopathological  
420 assessment. *JAMA Ophthalmol.* **132**, 338–345 (2014).
- 421 23. Pfau, M. *et al.* Determinants of cone- and rod-function in geographic atrophy: AI-based  
422 structure-function correlation. *Am. J. Ophthalmol.* **217**, 162–173 (2020).
- 423 24. Riedl, S. *et al.* The effect of pegcetacoplan treatment on photoreceptor maintenance in  
424 geographic atrophy monitored by AI-based OCT analysis. *Ophthalmol. Retin.* (2022).  
425 doi:10.1016/j.oret.2022.05.030
- 426 25. Thiele, S. *et al.* Natural history of the relative ellipsoid zone reflectivity in age-related  
427 macular degeneration. *Ophthalmol. Retin.* (2022). doi:10.1016/j.oret.2022.06.001
- 428 26. Schmitz-Valckenberg, S. *et al.* Fundus autofluorescence and fundus perimetry in the  
429 junctional zone of geographic atrophy in patients with age-related macular  
430 degeneration. *Investig. Ophthalmol. Vis. Sci.* **45**, 4470–4476 (2004).
- 431 27. Künzel, S. H. *et al.* Association of Reading Performance in Geographic Atrophy  
432 Secondary to Age-Related Macular Degeneration With Visual Function and Structural  
433 Biomarkers. *JAMA Ophthalmol.* **139**, 1191–1199 (2021).
- 434 28. Lindner, M. *et al.* Determinants of Reading Performance in Eyes with Foveal-Sparing  
435 Geographic Atrophy. *Ophthalmol. Retin.* **3**, 201–210 (2019).
- 436 29. Sunness, J. S. Reading newsprint but not headlines: pitfalls in measuring visual acuity  
437 and color vision in patients with bullseye maculopathy and other macular scotomas.  
438 *Retin. Cases Brief Rep.* **2**, 83–84 (2008).
- 439 30. Sunness, J. S. *et al.* The Long-term Natural History of Geographic Atrophy from Age-  
440 Related Macular Degeneration. Enlargement of Atrophy and Implications for  
441 Interventional Clinical Trials. *Ophthalmology* **114**, 271–277 (2007).
- 442 31. Pfau, M. *et al.* Green-Light Autofluorescence Versus Combined Blue-Light  
443 Autofluorescence and Near-Infrared Reflectance Imaging in Geographic Atrophy  
444 Secondary to Age-Related Macular Degeneration. *Invest. Ophthalmol. Vis. Sci.* **58**,  
445 BIO121–BIO130 (2017).
- 446 32. Holz, F. G. *et al.* Efficacy and safety of lomalizumab for geographic atrophy due to  
447 age-related macular degeneration: Chroma and spectri phase 3 randomized clinical  
448 trials. *JAMA Ophthalmol.* **136**, 666–677 (2018).
- 449 33. Schmitz-Valckenberg, S. *et al.* Semiautomated image processing method for  
450 identification and quantification of geographic atrophy in age-related macular

- 451 degeneration. *Investig. Ophthalmol. Vis. Sci.* **52**, 7640–7646 (2011).
- 452 34. Niu, S. et al. Automated retinal layers segmentation in SD-OCT images using dual-  
453 gradient and spatial correlation smoothness constraint. *Comput. Biol. Med.* **54**, 116–  
454 128 (2014).
- 455 35. Gorgi Zadeh, S. et al. CNNs enable accurate and fast segmentation of drusen in  
456 optical coherence tomography. in *Lecture Notes in Computer Science (including*  
457 *subseries Lecture Notes in Artificial Intelligence and Lecture Notes in Bioinformatics)*  
458 (eds. Cardoso, M. J. et al.) **10553 LNCS**, 65–73 (Springer International Publishing,  
459 2017).
- 460 36. Fang, L. et al. Automatic segmentation of nine retinal layer boundaries in OCT images  
461 of non-exudative AMD patients using deep learning and graph search. *Biomed. Opt.*  
462 *Express* **8**, 2732 (2017).
- 463 37. Maloca, P. M. et al. Validation of automated artificial intelligence segmentation of  
464 optical coherence tomography images. *PLoS One* **14**, e0220063 (2019).
- 465 38. Zweifel, S. A., Spaide, R. F., Curcio, C. A., Malek, G. & Imamura, Y. Reticular  
466 Pseudodrusen Are Subretinal Drusenoid Deposits. *Ophthalmology* **117**, 303–12.e1  
467 (2010).
- 468 39. Curcio, C. A. & Allen, K. A. Aging of the Human Photoreceptor Mosaic: Evidence for  
469 Selective Vulnerability of Rods in Central Retina. *Invest. Ophthalmol. Vis. Sci.* **34**,  
470 3278–3296 (1993).
- 471 40. Curcio, C. A., Medeiros, N. E. & Millican, C. L. Photoreceptor loss in age-related  
472 macular degeneration. *Investig. Ophthalmol. Vis. Sci.* **37**, 1236–1249 (1996).
- 473 41. Hill, A. B. The Environment and Disease: Association or Causation? *Proc. R. Soc.*  
474 *Med.* **58**, 295–300 (1965).
- 475 42. Takahashi, A. et al. Photoreceptor Damage and Reduction of Retinal Sensitivity  
476 Surrounding Geographic Atrophy in Age-Related Macular Degeneration. *Am. J.*  
477 *Ophthalmol.* **168**, 260–268 (2016).
- 478 43. Pfau, M. et al. Light sensitivity within areas of geographic atrophy secondary to age-  
479 related macular degeneration. *Investig. Ophthalmol. Vis. Sci.* **60**, 3992–4001 (2019).
- 480 44. Pfau, M. et al. Mesopic And Dark-adapted Two-color Fundus-controlled Perimetry In  
481 Geographic Atrophy Secondary To Age-related Macular Degeneration. *Retina* **40**,  
482 169–180 (2020).
- 483 45. Wu, Z. et al. Optical coherence tomography-defined changes preceding the  
484 development of drusen-associated atrophy in age-related macular degeneration.  
485 *Ophthalmology* **121**, 2415–2422 (2014).
- 486 46. Wu, Z. et al. Prospective Longitudinal Evaluation of Nascent Geographic Atrophy in  
487 Age-Related Macular Degeneration. *Ophthalmol. Retin.* **4**, 568–575 (2020).
- 488 47. Guymer, R. H. et al. Incomplete Retinal Pigment Epithelial and Outer Retinal Atrophy  
489 in Age-Related Macular Degeneration: Classification of Atrophy Meeting Report 4.  
490 *Ophthalmology* **127**, 394–409 (2020).
- 491 48. Wu, Z. et al. OCT Signs of Early Atrophy in Age-Related Macular Degeneration:  
492 Interreader Agreement: Classification of Atrophy Meetings Report 6. *Ophthalmol.*  
493 *Retin.* **6**, 4–14 (2022).
- 494 49. Nittala, M. G. et al. Association of Pegcetacoplan With Progression of Incomplete  
495 Retinal Pigment Epithelium and Outer Retinal Atrophy in Age-Related Macular  
496 Degeneration: A Post Hoc Analysis of the FILLY Randomized Clinical Trial. *JAMA*

- 497            *Ophthalmol.* (2022). doi:10.1001/jamaophthalmol.2021.6067
- 498    50.    Nittala, M. G. et al. Association of Pegcetacoplan With Progression of Incomplete  
499            Retinal Pigment Epithelium and Outer Retinal Atrophy in Age-Related Macular  
500            Degeneration: A Post Hoc Analysis of the FILLY Randomized Clinical Trial. *JAMA*  
501            *Ophthalmol.* (2022). doi:10.1001/jamaophthalmol.2021.6067
- 502    51.    Sadigh, S. et al. Abnormal thickening as well as thinning of the photoreceptor layer in  
503            intermediate age-related macular degeneration. *Investig. Ophthalmol. Vis. Sci.* **54**,  
504            1603–1612 (2013).
- 505    52.    Lu, C. D. et al. Photoreceptor layer thickness changes during dark adaptation  
506            observed with ultrahigh-resolution optical coherence tomography. *Investig.*  
507            *Ophthalmol. Vis. Sci.* **58**, 4632–4643 (2017).
- 508    53.    Jaffe, G. J. et al. C5 Inhibitor Avacincaptad Pegol for Geographic Atrophy Due to Age-  
509            Related Macular Degeneration: A Randomized Pivotal Phase 2/3 Trial.  
510            *Ophthalmology* **128**, 576–586 (2021).
- 511    54.    Jaffe, G. J. et al. Development of IONIS-FB-LRx to treat geographic atrophy  
512            associated with AMD. *Invest. Ophthalmol. Vis. Sci.* **61**, 4305 (2020).
- 513    55.    Khanani, A. M. et al. Phase 1 Study of the Anti-HtrA1 Antibody-binding Fragment  
514            FHTR2163 in Geographic Atrophy Secondary to Age-related Macular Degeneration.  
515            *Am. J. Ophthalmol.* **232**, 49–57 (2021).
- 516    56.    R Core Team. R: A Language and Environment for Statistical Computing. (2021).
- 517    57.    Wickham, H., François, R., Henry, L. & Müller, K. dplyr: A Grammar of Data  
518            Manipulation. (2021).
- 519    58.    Valero-Mora, P. M. *ggplot2: Elegant Graphics for Data Analysis*. *Journal of Statistical*  
520            *Software* **35**, (Springer, 2010).
- 521    59.    Bates, D., Mächler, M., Bolker, B. & Walker, S. Fitting Linear Mixed-Effects Models  
522            Using lme4. *J. Stat. Software; Vol 1, Issue 1* (2015).
- 523    60.    Lenth, R. V. emmeans: Estimated Marginal Means, aka Least-Squares Means. (2021).
- 524    61.    Martin Bland, J. & Altman, D. G. Statistical Methods for Assessing Agreement  
525            Between Two Methods of Clinical Measurement. *Lancet* **327**, 307–310 (1986).

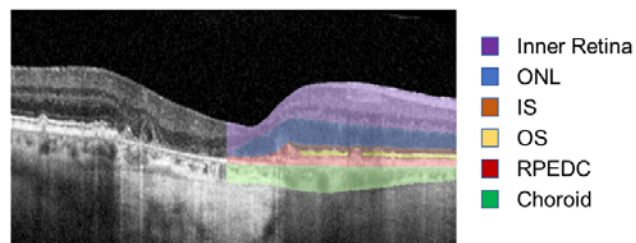
526 **FIGURES AND FIGURE LEGENDS**

527 **Figure 1. Image segmentation approach**

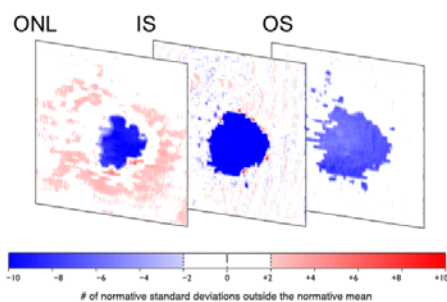
528 As shown in the first panel, all spectral-domain optical coherence tomography (SD-OCT)  
529 data were segmented using a convolutional neural network (CNN, Deeplabv3 model with a  
530 ResNet-50 backbone). Subsequently (second panel), these data were standardized (z-  
531 scores) to account for normal thickness variation due to age and retinal topography. Last  
532 (third panel), the retinal layers' thicknesses were extracted along evenly spaced contour-lines  
533 surrounding the retinal pigment epithelium (RPE) atrophy area. The yellow line denotes the  
534 boundary of RPE atrophy. The three purple lines represent the 0.43°, 2.58°, and 5.16°  
535 contour-lines.

536 **Abbreviations:** spectral-domain optical coherence tomography (SD-OCT), convolutional  
537 neural network (CNN), retinal pigment epithelium (RPE), outer nuclear layer (ONL),  
538 photoreceptor inner segments (IS), photoreceptor outer segments (OS), retinal pigment  
539 epithelium-drusen complex (RPEDC)

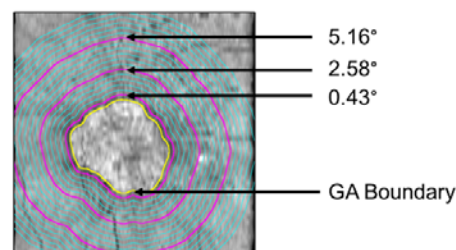
**A** SD-OCT Segmentation



**B** Standardization of Data



**C** Contour-Line-Based Analysis



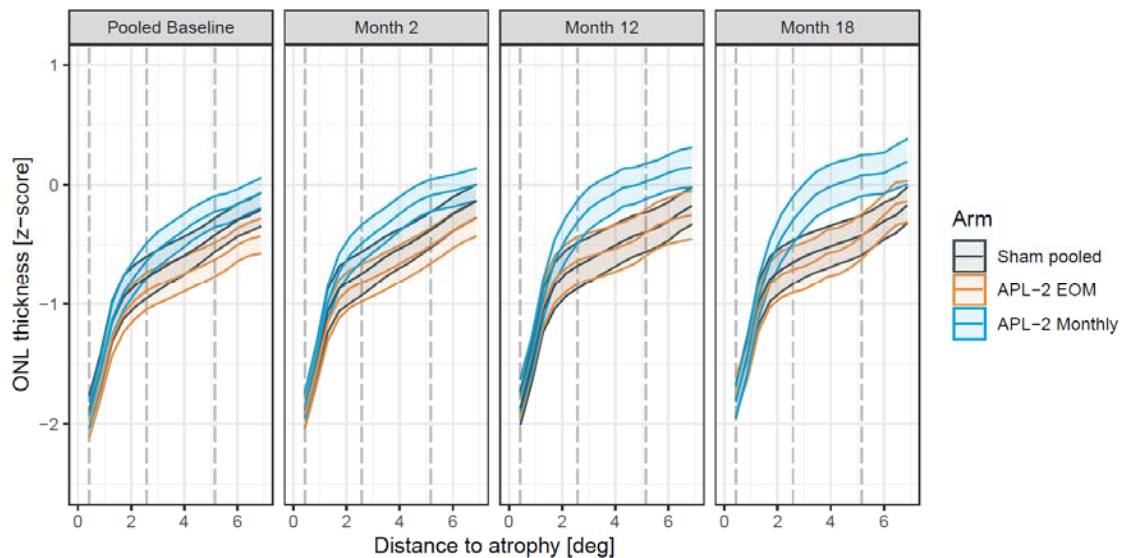
540  
541

542 **Figure 2. Change in thickness at the level of the outer nuclear layer (ONL) over time**

543 The plots show the average thickness at the level of the outer nuclear layer (ONL, y-axis)  
544 and the standard error of the mean (SEM, ribbons) with the distance to the boundary of  
545 retinal pigment epithelium (RPE) atrophy (x-axis). The panels indicate the visit, and the color  
546 indicates the treatment arm. The vertical dashed lines denote the 0.43°, 2.58°, and 5.16°  
547 contour-lines that were considered for the linear mixed model analyses. Please note that the  
548 baseline junctional-zone ONL thickness differed slightly among the groups. The actual  
549 contrasts (i.e., change-over-time from baseline) are shown in Figure 3.

550 The data were derived from the modified intention-to-treat (mITT) analysis ( $N_{\text{participants}}=192$ ).

551 **Abbreviations:** outer nuclear layer (ONL), photoreceptor inner segments (IS), photoreceptor  
552 outer segments (OS), modified intention-to-treat (mITT)



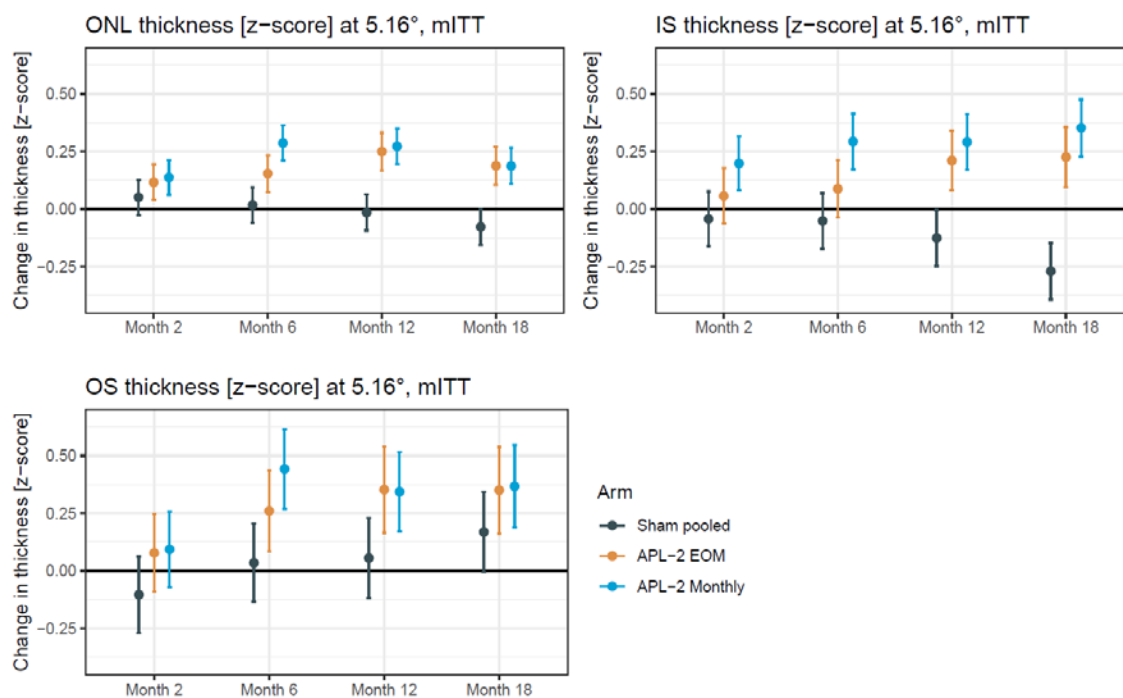
553

554 **Figure 3. Change in thickness at the level of the photoreceptor layers along the 5.16°**  
555 **contour-line over time, modified intention-to-treat (mITT) analysis**

556 The plots show the least-squares (adjusted) means from the linear mixed model analysis for  
557 the change in thickness at the level of the outer nuclear layer (ONL), photoreceptor inner  
558 segments (IS), and photoreceptor outer segments (OS) along the 5.16° contour-line as a  
559 function of the visit (x-axis) and treatment arm (colors). The vertical lines denote the 95%  
560 confidence intervals. Eyes treated with pegcetacoplan (APL-2) monthly tended to show a  
561 lesser degree of photoreceptor laminae thinning over time. Participants were treated  
562 between baseline and month 12.

563 The data were derived from the modified intention-to-treat (mITT) analysis ( $N_{\text{participants}}=192$ ).

564 **Abbreviations:** outer nuclear layer (ONL), photoreceptor inner segments (IS), photoreceptor  
565 outer segments (OS), modified intention-to-treat (mITT)



566



567 **TABLES**

568 **Table 1. Cohort characteristics for the included participants (modified intention-to-**  
 569 **treat [mITT] with Spectralis imaging)**

570 **Abbreviations:** retinal pigment epithelium (RPE), square-root (SQRT)

571

	Sham pooled (N=64)	APL-2 Monthly (N=67)	APL-2 EOM (N=61)	P-value for the between group difference*
<b>Age in years</b>				
Mean (SD)	78.0 (7.62)	80.1 (7.44)	80.3 (7.43)	0.16
Median [Min, Max]	78.0 [60.0, 96.0]	81.0 [63.0, 95.0]	80.0 [60.0, 97.0]	
<b>Sex</b>				
F	38 (59.4%)	44 (65.7%)	40 (65.6%)	0.71
M	26 (40.6%)	23 (34.3%)	21 (34.4%)	
<b>Laterality</b>				
L	31 (48.4%)	27 (40.3%)	20 (32.8%)	0.21
R	33 (51.6%)	40 (59.7%)	41 (67.2%)	
<b>Study eye SQRT- transformed area of RPE- atrophy in mm</b>				
Mean (SD)	2.78 (0.725)	2.75 (0.663)	2.88 (0.772)	0.60
Median [Min, Max]	2.65 [1.60, 4.07]	2.74 [1.59, 4.16]	3.00 [1.59, 4.12]	

572 \* Between-group differences in continuous variables (age and sqrt. area of atrophy) were evaluated with an  
 573 ANOVA, and Fisher's exact test was applied for categorical data (sex and laterality).

574 **Table 2. Study eye differences in thickness at the level of photoreceptor layers (in z-score units) at three contour-lines at month 12**  
 575 **(modified intention-to-treat [mITT] analysis)**

Layer	Contrast	0.43°			2.58°			5.16°		
		Estimate	95% CI	P-value*	Estimate	95% CI	P-value*	Estimate	95% CI	P-value*
ONL	(APL-2 Monthly) - Sham pooled	0.1	[-0.03, 0.24]	.16	0.26	[0.14, 0.38]	<.001	0.29	[0.16, 0.42]	<.001
ONL	(APL-2 EOM) - Sham pooled	0.12	[-0.01, 0.26]	.09	0.16	[0.04, 0.29]	.006	0.26	[0.13, 0.4]	<.001
ONL	(APL-2 Monthly) - (APL-2 EOM)	-0.02	[-0.15, 0.12]	.95	0.09	[-0.03, 0.22]	.17	0.02	[-0.11, 0.16]	.92
IS	(APL-2 Monthly) - Sham pooled	0.68	[0.09, 1.28]	.02	0.48	[0.21, 0.75]	<.001	0.42	[0.21, 0.62]	<.001
IS	(APL-2 EOM) - Sham pooled	1.09	[0.48, 1.71]	<.001	0.4	[0.12, 0.68]	.002	0.34	[0.12, 0.55]	<.001
IS	(APL-2 Monthly) - (APL-2 EOM)	-0.41	[-1.02, 0.2]	.26	0.08	[-0.2, 0.36]	.78	0.08	[-0.13, 0.29]	.64
OS	(APL-2 Monthly) - Sham pooled	-0.09	[-0.38, 0.19]	.72	0.18	[-0.12, 0.48]	.33	0.29	[-0.01, 0.58]	.06
OS	(APL-2 EOM) - Sham pooled	0.05	[-0.24, 0.35]	.9	0.52	[0.21, 0.83]	<.001	0.3	[-0.01, 0.6]	.06
OS	(APL-2 Monthly) - (APL-2 EOM)	-0.15	[-0.44, 0.14]	.45	-0.34	[-0.64, -0.03]	.03	-0.01	[-0.31, 0.3]	1

576

577 \* P-values were obtained using Kenward-Roger approximation to estimate the denominator degrees of freedom. P-values were adjusted within  
 578 each model (i.e., combination of layer and contour-line) using the Tukey method for comparing a family of 3 estimates.